International Journal of Navigation and Port Research
Vol.27, No.3 pp. 253~258, 2003 (ISSN-1598-5725)

# The Prediction of Hydrodynamic Forces Acting on Ship Hull in Laterally Berthing Maneuver Using CFD

*Yun-Sok Lee*

* *Kobe University of Mercantile Marine, Kobe, Japan*

**Abstract** : *To evaluate the unsteady motion in laterally berthing maneuver, it is necessary to grasp very clearly the magnitude and properties of the hydrodynamic forces acting on ship hull in shallow water. In this study, numerical calculation was made to investigate quantitatively the hydrodynamic force according to the water depth for Wigley model using the CFD (Computational Fluid Dynamics) technique. Comparing the computational results to the experimental ones, the validity of the CFD method was verified. The numerical solutions evaluated the hydrodynamic force with good accuracy, and then captured the features of the flow field around the ship in detail. The transitional lateral force in a state ranging from rest to uniform motion is modeled by using the concept of the circulation.*

**Key words** : *Berthing Maneuver, Hydrodynamic Force, Transitional Lateral Force, CFD, Shallow Water*

## 1. Introduction

The berthing maneuver is a specific work keeping allowance strength of the mooring facilities in addition to the safety of the vessel itself. The accurate position and control of the vessel are required with the aid of tugboats. One of problems in a berthing maneuver is that the magnitude and features of the hydrodynamic force acting on ship hull as a function of water depths and ship types have not been analyzed clearly. In typical berthing motion such as large tanker vessel, the berthing maneuver is usually executed in low lateral moving velocity and in the short distance to the berth. But considerable force will act on ship hull because it is not a streamlined form to the moving direction. In such motion, the transitional lateral force is subjected to the position and strength of the separated vortices. Moreover since the hydrodynamic forces differ greatly according to their kinetic history even at the same velocity, the force cannot be dealt with steady or quasi steady condition. The transitional lateral force appears strongly, and remains for a very long time in the shallow water.

It is assumed that the hydrodynamic force can be simply divided into inertia force and lateral force. Concerning with the inertia force such as added mass, we already proposed the simplified formulas expressed in the water depth and the type of ships(Lee, Y. S., Sadakane, H. and Toda, Y. 2000). With lateral force, we also proposed an estimation formula based on the model experiment(Sadakane, H. 1996), Meanwhile in case that complicated hydrodynamic force is to be dealt with, not only just estimation of the hydrodynamic force, but also hydrodynamic comprehension concerning the mechanisms of the hydrodynamic force becomes necessary. The experiment cannot satisfy these requirements.

In this paper, we used the CFD(Chen, M. and Chen, H. C. 1996, Toda, Y., Lee, Y. S. and Sadakane, H. 2002, Toda, Y., Lee, Y. H. and Sadakane, H. 2002), (Computational Fluid Dynamics) which is effective to visually observe the detailed characteristics of the flow field. The numerical calculations and the experiments are carried. The validity of CFD method is evaluated. This study is the basic research to obtain quantitatively the hydrodynamic forces under the lateral motion by use of the CFD technique, and to generalize the obtained hydrodynamic forces for practical use.

## 2. Outline of Numerical Method

The berthing velocity of a large tanker aided by tugboat operation in harbor is usually less than 0.15m/s, and the Froude Number *Fn* determined by taking the ship breadth is very small values. Based upon these facts, influence of the free surface was neglected on the computation. The motion mode during the lateral moving used for the computation corresponds to CAT (Constant Acceleration Test) starting from rest to constant acceleration, to uniform movement, to constant deceleration, and to stop.

### 2.1 Governing equation and turbulence model

The governing equations are the continuity and Naiver-Stokes equations for viscous incompressible flow written in the physical domain using Cartesian coordinate

* Corresponding Author : Yun-Sok Lee, yunsok@kshosen.ac.jp 051)410-4863

fixed on ship hull. All variables are normalized by means of breadth $B$, reference velocity $U_\infty$ (the uniform velocity), fluid density $\rho$, and combination of these factors.

The SGS (Sub-Grid Scale) turbulence model seems to be suitable for the unsteady and complicated flow field with the shedding vortex and relatively rough computational grid. The eddy viscosity $(\upsilon_t = 1/R_e + \upsilon_s)$ of Smagorinsky is used and $\upsilon_s$ is determined by a Takakuras length scale (Takakura, Y., Ogiwara, S. and Isiguro, T. 1989, Watanabe, O., Ming, Z. and Miyata, H. 1992). The non-dimensional equations are transformed into the computational domain in non-orthogonal curvilinear coordinate. A partial transformation is used in which only the independent variables are transformed. Each equation is generally rewritten in the form of the convection/diffusion equation as follow:

$$\frac{1}{J}\sum_{i=1}^{3}\sum_{j=1}^{3}\frac{\partial}{\partial \xi^i}\left(b_i^j U_j\right) = 0 \tag{1}$$

$$\sum_{i=1}^{3}\sum_{j=1}^{3} g^{ij}\frac{\partial^2\phi}{\partial\xi^i\partial\xi^j} - 2\sum_{j=1}^{3} a_\phi^j\frac{\partial\phi}{\partial\xi^j} = R_\phi\frac{\partial\phi}{\partial\tau} + S_\phi \tag{2}$$

The transport equations are discretized using the 12 point finite analytic method(Patel, V.C, Chen, H.C. and Ju, S. 1990, Tahara, Y. 1993). In the finite-analytic scheme, equation is linearlized in each local numerical elements and solving analytically by the method of separation of variables. Euler implicit method is applied to the time derivatives. Pressure-velocity coupling is accomplished using the PISO algorithm(Chen, H.C. and Korpus, R. 1993). Therefore hundred times of repetition is required for every trial of the calculation of one-time step, the coefficient of the FA method was renewed every time repetition.

### 2.2 Computational Grid and Boundary Conditions

The present computational grid is H-type with constant $Y$ planes, which is generated by solving the Possion equation. Coordinate system and computational grid of Wigley hull is shown in Fig. 1. The origin is at the water surface and midship section. $X$ is the opposite direction for the movement, $Y$ is the ship length direction and $Z$ is directed vertically downward. Length and draft are normalized by breadth. So, the length is 10, breadth is 1, and draft is 0.625. The computational gird number is 81×95×35 in directions of x, y, and z in case of the deep water region. In case that H/d is 2.0 and 1.5, computation was conducted by reducing exclusively the $Z$ axis to 19 and 21. Fig. 2 shows the computational gird on the water surface plane. The boundary condition are given in the shallow water region as follows: the inlet boundary condition (x =-30); $u = U_0$, $v = w = p = 0$, the outlet boundary condition (x = 30, 0 extrapolation); $\partial u/\partial x = \partial v/\partial x = \partial w/\partial x = \partial p/\partial x = 0$, the side(right and left) boundary condition (y = ± 25); $u = U_0$ , $v = w = p = 0$. Furthermore the boundary condition on the hull surface was approximated with $u = v = w = 0$, $\partial p/\partial x = dU_0/dt$. Body hull is located $-5 \leqq y \leqq 5$, $-0.5 \leqq x \leqq 0.5$. Non- dimensional acceleration and deceleration for computation is $\pm 1$ $(dU_0/dt = \pm 1)$. The Reynolds number was designated as 105 considering the Reynolds number of the experiment, and the non-dimensional time interval of 1 step is $\Delta t = 0.005$ (200 steps are equivalent to the non-dimensional time T = 1.0).

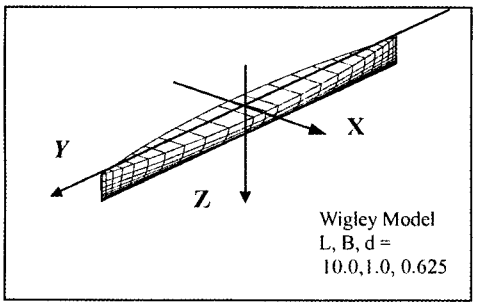


Fig. 1 Coordinate system and computational grid.

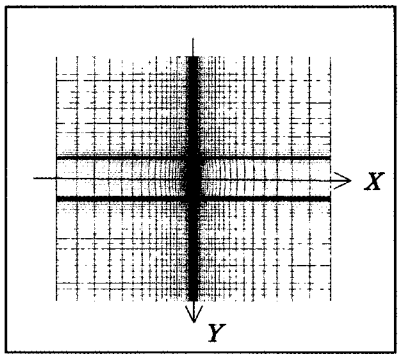


Fig. 2 Computational grid on the water plane.

## 3. Numerical Results

### 3.1 Change in the hydrodynamic force according to water depth

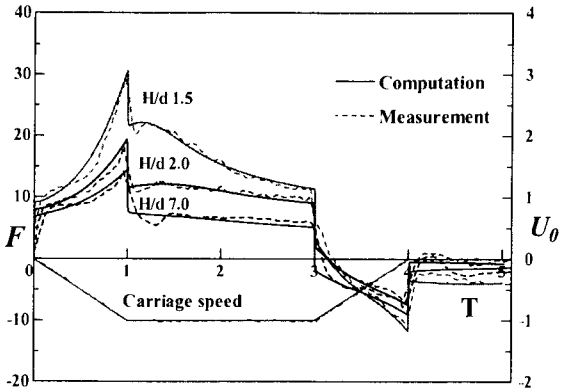


Fig. 3 Comparision of hydrodynamic forces.

The comparison of the hydrodynamic force between computations and experiments according to the water depth, such as H/d=2.0, 1.5 and H/d=7.0 is shown in Fig. 3. The force $F$ and moving velocity $U_0$ in Fig. 3 are the normalized values, and the non dimensional acceleration is 1.0. The solid line gives the computation result, whereas the dotted line gives the experimental result obtained by using a lateral force measurement device. In order to compare both of the hydrodynamic forces directly, inertia force corresponding to the model mass used in the experiment was added to the CFD results. The experimental result in Fig. 3 is obtained by means of lateral force measurement equipment using a servo motor control, as shown in Fig. 4. The equipment can run within 1.0m, and the carriage speed and acceleration are set freely on the personal computer. It is shown that the CFD result is satisfactory enough to coincide with the experimental result. Thus it is validated that the hydrodynamic force obtained from the CFD method can be estimated with sufficient accuracy. Also, the force in Fig. 3 is almost pressure component, and the viscosity stress component is small enough to be ignored. As a feature of the hydrodynamic force caused by the difference of the water depth, especially the transitional lateral force under the uniform movement is showed largely as the force comes to shallower water. Furthermore a feature came to manifest itself remarkably with the decrease of the force in a short time. The added mass concerning the inertia component appearing just after the acceleration and just before the deceleration was found to be almost the same in its magnitude despite the great difference of the flow field around the ship. Also utilizing the merit of CFD computation, change of the flow field dependent on water depth is hereby observed. Instantaneous streamlines of water surface plane in case that H/d=2.0 and 1.5 are shown in Fig. 5, respectively. Since the flow comes to be hard to go through the ship bottom, a flow running around the fore and aft makes remarkable appearance in shallow water. Therefore it is shown that great positive pressure is worked on the front of the hull in a shallow region. From the visualized information, the influence on the flow field around the ship hull can very easily be explained. Thus it can be ensured that the water depth is an important element to affect in fluence on the hydrodynamic force, and it has become possible to compare and examine the hydrodynamic force in detail based on the CFD computation result.

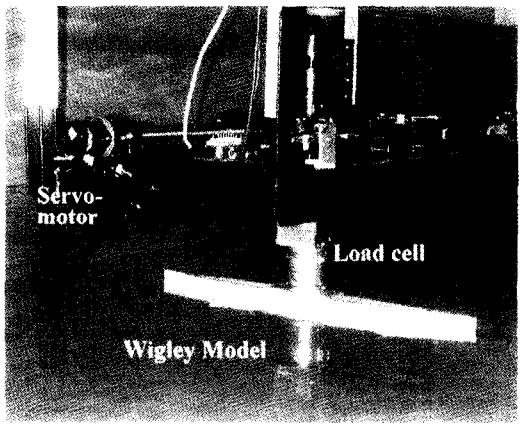


Fig. 4 Configuration of Experiment.

### 3.2 Change in the hydrodynamic force according to the acceleration

In undergoing laterally berthing maneuver, the ship makes lateral moving with the support of a tugboat, but acceleration movement is made with the hull from rest to

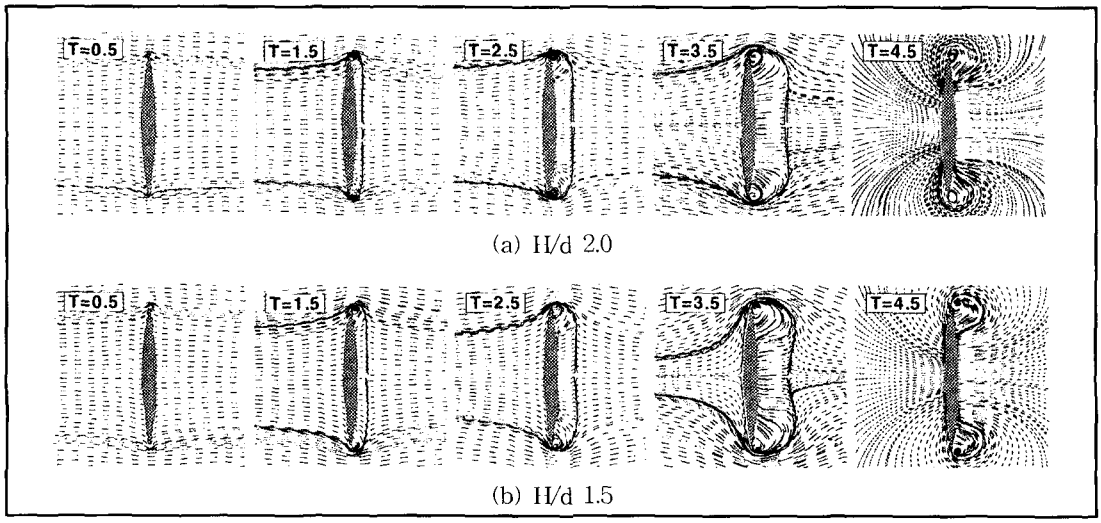


Fig. 5 Instantaneous streamlines of water surface(relative velocity to the hull).

uniform movement. Thus change of the flow field influenced by the difference of the acceleration movement depending on the number of the tugboat and the power of the tugboat is hereby examined. Even if the lateral moving velocity is the same, it is considered that the hydrodynamic forces acting on ship hull according to the difference of the acceleration is greatly different. To examine the change of the hydrodynamic force effected by the difference of the acceleration, computation was made from rest to uniform movement T = 5.0 using the CFD method in case that H/d = 7.0 where the water depth is deep enough and H/d = 1.5 where the water depth is relatively shallow taking up the 3 types of different non-dimensional acceleration (i.e., NDA 0.5, 1.0, and 2.0). Computational result of hydrodynamic forces according to the acceleration is compared with experiment result in Fig. 6 (H/d=7.0) and Fig. 7 (H/d=1.5), respectively. From the Fig. 6 & 7, it is confirmed that the CFD results is in coincidence with the experiment with good accuracy. Thus it might be possible to evaluate the hydrodynamic force by the use of CFD.

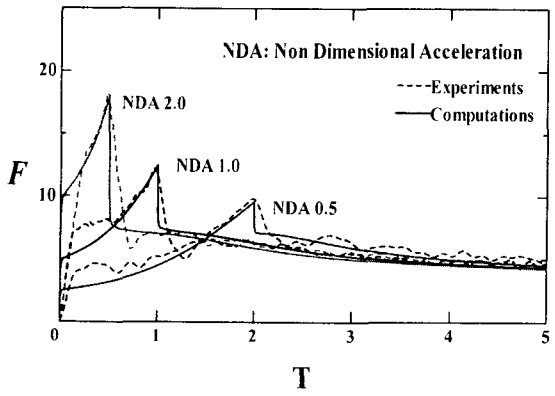


Fig. 6 Comparison of hydrodynamic forces according to the acceleration (H/d 7.0).

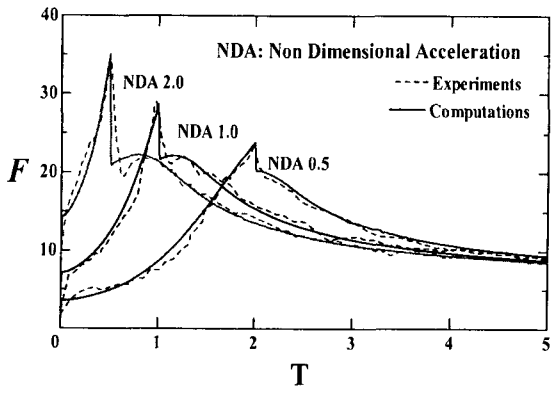


Fig. 7 Comparison of hydrodynamic forces according to the acceleration (H/d 1.5).

Let the hydrodynamic force under the lateral moving of the ship hull can be classified into inertia force and lateral force. The inertia force in case that NDA is 2.0 was twice as large as the force in case that NDA is 1.0. The inertia force in case that NDA is 0.5 was half of the one referred to above. In case that NDA is 1.0, the inertia force in a deep water H/d = 7.0 was 4.8, whereas the value was 7.2 in a shallow H/d = 1.5. Thus it is ensured that among the hydrodynamic forces subjected to the difference of the acceleration, the inertia force becomes larger which is dependent exclusively on the acceleration.

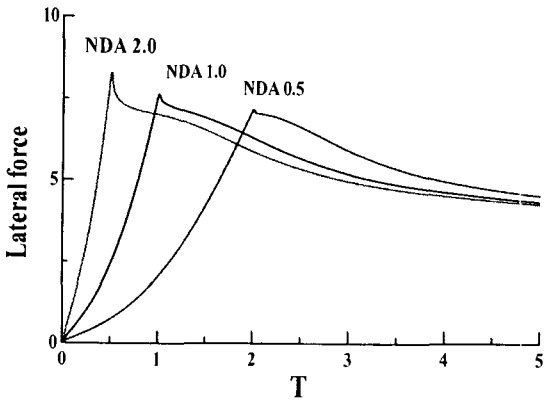


Fig. 8 Comparison of lateral drag force(H/d 7.0).

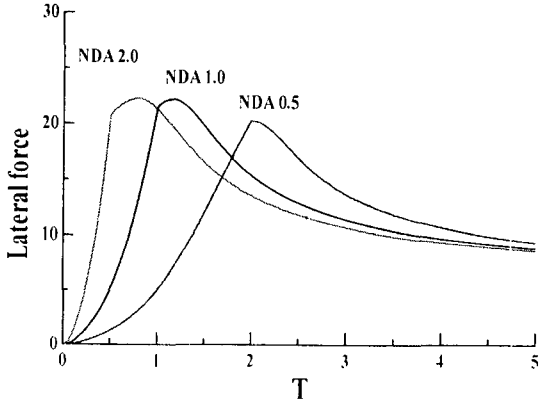


Fig. 9 Comparison of lateral drag force(H/d 1.5).

The lateral force obtained by deducting inertia force from computational results of the CFD is shown in Fig. 8 and 9. Comparing Fig. 8 with Fig. 9, the lateral force becomes approximately 3 times larger at H/d = 1.5 than at H/d = 7.0 and is greatly susceptible to the influence of the shallow water. Meanwhile as long as the water depth was the same, almost none of difference was noticed with the maximum value (just after acceleration) caused by the difference of the acceleration. However the tendency of transitional lateral force was slightly different. In case that the water depth is shallow (H/d =1.5), the lateral force was increased for a while just after starting the uniform movement. Such features remarkably appeared when the acceleration is very high.

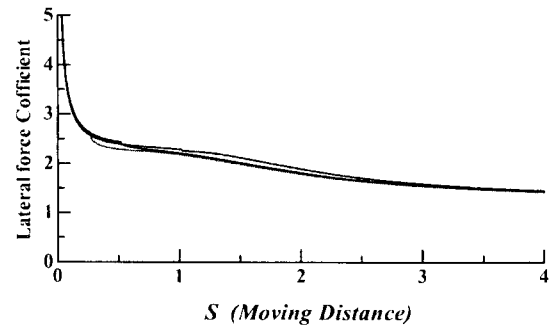


Fig. 10 Lateral drag coefficient according to the moveing distance when H/d = 7.0.

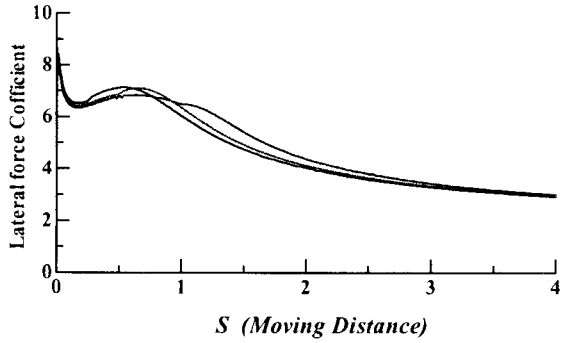


Fig. 11 Lateral drag coefficient according to the moveing distance when H/d = 1.5.

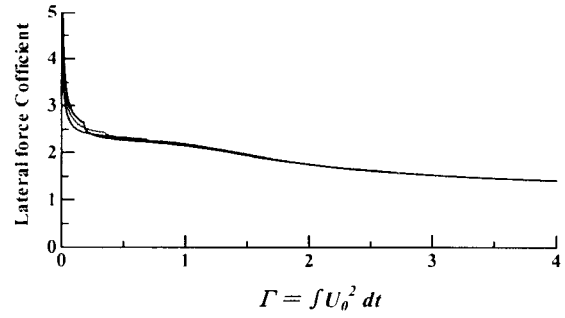


Fig. 12 Lateral drag coefficient according to the circulation when H/d = 7.0.

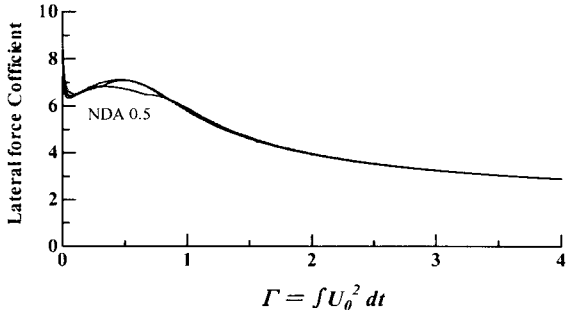


Fig. 13 Lateral drag coefficient according to the circulation when H/d = 1.5.

## 4. Modeling of Lateral Drag Force

The lateral force ranging from a resting state to uniform movement is aligned according to the lateral moving distance of the hull based on a report by Sadakane et al(Tahara, Y., 1993), (Chen, H.C. and Korpus, R., 1993), Details of the above are shown in Fig. 10 (H/d=7.0) and Fig. 11 (H/d=1.5). The abscissa of both the figures correspond to the lateral moving distance S, whereas the ordinate comply with the transitional lateral force coefficient $C_{wy}$ ($C_{wy}$ = $F/0.5\rho LU_0^2$). First in case of Fig.10 indicating the deep water, slight difference is noted, but totally good agreement is seen. However in case of H/d = 1.5 where the water depth is relatively shallow, the tendency is quite different from the one in case of the deep water. Especially in case that S < 3.0, disagreement is noted. That is to say, it is almost impossible to align the lateral force by means of exclusively the lateral moving distance.

As a method to express the transitional lateral force quantitatively, modeling of the transitional lateral force coefficient is attempted by introducing the concept of circulation as a variable closely related with the magnitude and development of the vortex surrounding the hull. From the fact that the velocity of the separated vortex is in proportion to the lateral moving velocity $U_0$ of the hull, the function of circulation is expressed using the lateral moving velocity and moving distance(Lee, Y. S. 2003), as follows:

$$\Gamma = \int uds \propto \int U_0^2 \, dt \tag{3}$$

The transitional lateral force coefficient obtained by taking the Eq. (3) is shown in Fig. 12 and 13. They comply with the lateral coefficient in case that H/d is 7.0 and 1.5, respectively. Comparing Fig. 12 and 13 with Fig. 10 and 11, it is found that it is possible to use circulation in case of both the deep water and the shallow water. However in case of the shallow water as shown in Fig. 13, the one exclusively with NDA 0.5 becomes smaller than the other ones in the vicinity of $S=0.5$. Using the circulation obtained by multiplying the lateral moving velocity of the hull with its moving distance, it is considered that modeling of the lateral force coefficient ranging from a resting state to uniform movement becomes possible. Investigation for modeling to describe the transitional lateral force coefficient of real ship except Wigley is required.

## 5. Conclusion

By applying the 3-dimensional CFD method to the Wigley hull, unsteady hydrodynamic force was obtained. The results of this paper can be summarized as follows:

(1) The CFD computation result is finely in agreement with the experimental result, and it is ensured that the unsteady hydrodynamic force under the laterally berthing maneuver can be estimated with sufficient accuracy by CFD technique.
(2) It is ensured that water depth is an important factor to exercise influence on the inertia force and transitional lateral force acting on ship hull.
(3) The added mass in case of acceleration and deceleration was almost of the same magnitude despite the difference of the fluid field surrounding the hull.
(4) The transitional lateral force in a state ranging from rest to uniform motion is modeled by using the concept of the circulation, which is obtained by multiplication of the lateral moving distance and moving velocity.

These results provide useful information for safe ship operation, ship-handling simulators, structure strengthening of berths, design of fenders and rational assessment of required horse power of etc. tugboat,

## References

[1] Chen, H.C. and Korpus, R. (1993), A Multi-block Finite-Analytic Reynolds-Averaged Navier-Stokes Method for 3D Incompressible Flows , Individual Papers in Fluid Engineering, edited b F. M. White, ASME FED-Vol. 150, ASME Fluids Engineering Conference, pp. 113-121.
[2] Chen, M. and Chen, H. C. (1996), Numerical Simulation of Transitional Flows Induced by a Berthing Ship, International Journal of Offshore and Polar Engineering, ISOPE, Vol. 7, No.4, pp. 277-284.
[3] Lee, Y. S. (2003), A Study on the Maneuvering Hydrodynamic Forces for Berthing Using CFD Technique, Ph. D. Thesis, Dept. Maritime Science, Kobe University of Mercantile Marine.
[4] Lee, Y. S., Sadakane, H. and Toda, Y. (2000), Hydrodynamic Forces Acting on a Ship Hull Under Lateral Low Speed Motion, Journal of the Japan Institute of Navigation, No. 102, pp. 87-95.
[5] Patel, V.C, Chen, H.C. and Ju, S. (1990), Ship Stern and Wake Flows: Solutions of the Fully-Elliptic Reynolds-Averaged Navier-Stokes Equations and Comparisons with Experiments, Journal of Computational Physics, Vol. 88, No.2, pp. 305-336.
[6] Sadakane, H. (1996), A Study on Lateral Drag Coefficient for Ship Moving Laterally from Rest, Journal of the Japan Institute of Navigation, No. 95, pp. 193-200.
[7] Tahara, Y. (1993), Computation of Viscous Flow around Series 60 Model and Comparison with Experiments , Journal of The Kansai Society of Naval Architects, No.220, pp. 29-47.
[8] Takakura, Y., Ogiwara, S. and Isiguro, T. (1989), Turbulence Models for Transonic Viscos Flow, AIAA paper, 89-1952 CP.
[9] Toda, Y., Lee, Y. S. and Sadakane, H. (2002), Hydrodynamic Forces Acting on a Ship Hull Under Lateral Low Speed Motion - Basic Consideration Using 3-D CFD Technique- , Journal of the Japan Institute of Navigation, No. 106, pp. 87-95.
[10] Toda, Y., Lee, Y. H. and Sadakane, H. (2002), Numerical Investigations of Hydrodynamic Forces Acting on a Ship Hull under Lateral Low Speed Motion , Journal of the kansai society of naval architects, No. 238, pp. 77-83.
[11] Watanabe, O., Ming, Z. and Miyata, H. (1992), Numerical Simulation of a Viscous Flow with Free-Surface Wave about a Ship by a Finite-Volume Method , Journal of The Society of Naval Architects of Japan, No.171, pp.27-39.

**Received** 30 May 2003
**Accepted** 14 August 2003